Determination of the linear coupling resonance strength using two-dimensional invariant tori

J. Y. Liu, M. Ball, B. Brabson, J. Budnick, D. D. Caussyn, V. Derenchuk, G. East, M. Ellison, D. Friesel, B. Hamilton, H. Huang, W. P. Jones, S. Y. Lee, D. Li, K. Y. Ng,* A. Riabko, T. Sloan, and Y. Wang
Indiana University Cyclotron Facility, Indiana University, Bloomington, Indiana 47405
(Received 20 September 1993)

Experimentally obtained Poincaré maps in the resonant rotating frame for particle motion with linear coupling revealed invariant tori of the two-dimensional Hamiltonian. Using these tori, we obtained the linear coupling strength, the tune shift with betatron amplitude coefficients, and the proximity parameter to the resonance. The coupling strength obtained with this method agreed well with that obtained from measuring the betatron tune separation of the normal modes.

PACS number(s): 41.85.−p, 03.20.+i, 05.45.+b, 29.20.Dh

I. INTRODUCTION

Almost all synchrotrons encounter problems related to the linear betatron coupling between the horizontal and vertical motion, which can arise from skew quadrupoles, vertical closed-orbit deviation in sextupoles, and solenoidal fields. The effects of linear coupling on the beam dynamics are betatron tune shifts, beating between the horizontal and vertical betatron oscillations, induced vertical dispersion, emittance dilution, and reduction of the dynamical aperture. Thus linear coupling can lead to performance degradation of colliders and storage rings. On the other hand, a controlled amount of linear coupling can be helpful in achieving a desirable vertical emittance for electron storage rings.

The horizontal and vertical deviations from the closed orbit of a beam particle satisfy Hill's equation [1]:

$$\frac{d^2x}{ds^2}+K_x(s)x=\frac{\Delta B_z}{B\rho},\quad \frac{d^2z}{ds^2}+K_z(s)z=-\frac{\Delta B_x}{B\rho}.$$

Here $K_x(s), K_z(s)$ are focusing functions due to quadrupoles, $B\rho$ is the magnetic rigidity, s is the longitudinal particle coordinate, and ΔB_x and ΔB_z are linear or nonlinear magnetic multipole field errors. In the linear approximation, the solution of the error-free Hill's equation is

$$y=\sqrt{2\beta_y(s)J_y}\cos(\phi_y+\psi_y(s)-\nu_y\theta),$$

where $\beta_y(s)$ is the betatron amplitude function, (J_y,ϕ_y) are the conjugate action-angle variables, $\psi_y(s)=\int_{s_0}^{s}\frac{ds}{\beta_y}$ is the betatron phase advance relative to a reference point s_0, $\nu_y=\frac{1}{2\pi}\oint\frac{ds}{\beta_y}$ is the number of betatron oscillations in one revolution and is called the betatron tune, $\theta=(s-s_0)/R$ is the orbital angle, while R is the average radius of the accelerator. Here y stands for either x or z. Thus particles are executing *betatron oscillations* transversely about the closed orbit of an accelerator.

The linear coupling resonances, which couple the horizontal and the vertical betatron oscillations, are located at $\nu_x\pm\nu_z=l$. This paper studies the linear difference-coupling resonance. The magnitude C and the phase χ of the coupling constant for the linear difference-coupling resonance $\nu_x-\nu_z=l$ are given by [2]

$$Ce^{i\chi}=\frac{1}{2\pi}\int_{s_0}^{s_0+2\pi R}\sqrt{\beta_x\beta_z}A_{xz}(s)\times e^{i[\psi_x-\psi_z-(\nu_x-\nu_z-l)\theta]}ds, \quad (1)$$

where

$$A_{xz}(s)=\left[\frac{1}{B\rho}\frac{\partial B_z}{\partial z}-\frac{B_\parallel}{4B\rho}\left(\frac{1}{\beta_x}\frac{d\beta_x}{ds}-\frac{1}{\beta_z}\frac{d\beta_x}{ds}\right)-i\frac{B_\parallel}{2B\rho}\left(\frac{1}{\beta_x}+\frac{1}{\beta_z}\right)\right].$$

Here $\frac{\partial B_z}{\partial z}/B\rho$ and $B_\parallel/B\rho$ are respectively the skew quadrupole and the solenoidal field strengths.

For betatron motion with linear coupling in two degrees of freedom (2D), the equations of motion can be decoupled into two normal modes [3]. The measured betatron tunes correspond to the eigenvalues of these normal modes. Traditionally, the linear coupling is measured and corrected by minimizing the separation between the betatron tunes of normal modes with combos of quadrupoles and skew quadrupoles. The magnitude of the coupling constant is given by the minimum tune separation between these two eigenmodes, which is also characterized by the beat period of the horizontal and the vertical betatron oscillations. However, this method fails to determine the phase of the linear coupling. For accelerators with periodic focusing and defocusing (FODO) cell structure, the linear coupling constant is dominantly real. On the other hand, the linear coupling constant may contain a substantial imaginary part due to solenoidal

*Permanent address: Fermilab, P.O. Box 500, Batavia, IL 60510.

field and/or large local phase difference between the horizontal and vertical phase advances at the low-β insertion section for high energy colliders and storage rings. Therefore the task of developing methods for measuring both the strength and the phase of the linear coupling is important.

This work is intended to study a method of measuring the magnitude and the phase of the linear coupling by using the 2D torus for the Poincaré surface of sections derived from experimental data. Section II discusses properties of the linear-coupling Hamiltonian. Section III deduces invariant tori for the linear coupling Hamiltonian from experimental data. The conclusion is given in Sec. IV.

II. HAMILTONIAN FOR LINEAR BETATRON COUPLING

By transforming the phase space coordinates into the action-angle variables, the Hamiltonian describing the betatron motion, in the presence of linear coupling, can be approximated by

$$H = \nu_x J_x + \nu_z J_z + \frac{1}{2}\alpha_{xx} J_x^2 + \alpha_{xz} J_x J_z + \frac{1}{2}\alpha_{zz} J_z^2 + C\sqrt{J_x J_z}\cos(\phi_x - \phi_z - l\theta + \chi), \quad (2)$$

where ν_x and ν_z are the linear betatron tunes, J_x, ϕ_x, J_z, and ϕ_z are, respectively, the action-angle variables for the horizontal and vertical betatron motions, α_{xx}, α_{xz} and α_{zz} are the nonlinear betatron detuning parameters, and C and χ are the strength and phase of the linear coupling constant given by Eq. (1).

We transform the Hamiltonian into the resonant precessing frame by using the generating function

$$F_2(\phi_x, \phi_z, J_1, J_2) = (\phi_x - \phi_z - l\theta + \chi)J_1 + \phi_z J_2,$$

to obtain new action-angle variables given by $\phi_1 = \phi_x - \phi_z - l\theta + \chi$, $\phi_2 = \phi_z$, $J_1 = J_x$ and $J_2 = J_x + J_z$. The new Hamiltonian can be decomposed into $H = H_1(J_1, \phi_1, J_2) + H_2(J_2)$ with

$$H_1 = \delta_1 J_1 + \frac{1}{2}\alpha_{11} J_1^2 + C\sqrt{J_1(J_2 - J_1)}\cos\phi_1, \quad (3)$$

and $H_2(J_2) = \nu_z J_2 + \frac{1}{2}\alpha_{zz} J_2^2$, where $\delta_1 = \nu_x - \nu_z - l + (\alpha_{xz} - \alpha_{zz})J_2$ is the resonance proximity parameter observed from the *horizontal action variable*, and $\alpha_{11} = \alpha_{xx} - 2\alpha_{xz} + \alpha_{zz}$ is the effective nonlinear detuning parameter at the resonance. There are two invariants for the motion, i.e., J_2 and H. Hamilton's equations of motion are given by

$$\dot{J}_1 = C\sqrt{J_1(J_2 - J_1)}\sin\phi_1, \quad (4)$$

$$\dot{\phi}_1 = \delta_1 + \alpha_{11} J_1 + C\frac{J_2 - 2J_1}{2\sqrt{J_1(J_2 - J_1)}}\cos\phi_1. \quad (5)$$

The particle motion in the resonant rotating frame is determined completely by the condition of a constant J_2 and a constant Hamiltonian value $H_1(J_1, \phi_1, J_2) = E$. These tori depend only on two parameters, $b = \frac{\delta_1}{\alpha_{11} J_2}$ and $c = \frac{C}{\alpha_{11} J_2}$. Examples of tori for the Hamiltonian H_1 are shown with parameters $J_2 = 1$ (π-mm-mrad) and $b = 0, c = 0.25$ in Fig. 1(a), $b = -0.5, c = 0.25$ in Fig. 1(b), and $b = -0.5, c = 0.5$ in Fig. 1(c), respectively, where we have used the normalized coordinates $Q = \sqrt{2J_1}\cos\phi_1$, $P = -\sqrt{2J_1}\sin\phi_1$.

The fixed points of the Hamiltonian are given by the conditions $\dot{J}_1 = 0$ and $\dot{\phi}_1 = 0$. There are, in general, two or four possible fixed points at $\phi_1 = 0$ or π with

$$\delta_1 + \alpha_{11} J_1 \pm C\frac{J_2 - 2J_1}{2\sqrt{J_1(J_2 - J_1)}} = 0. \quad (6)$$

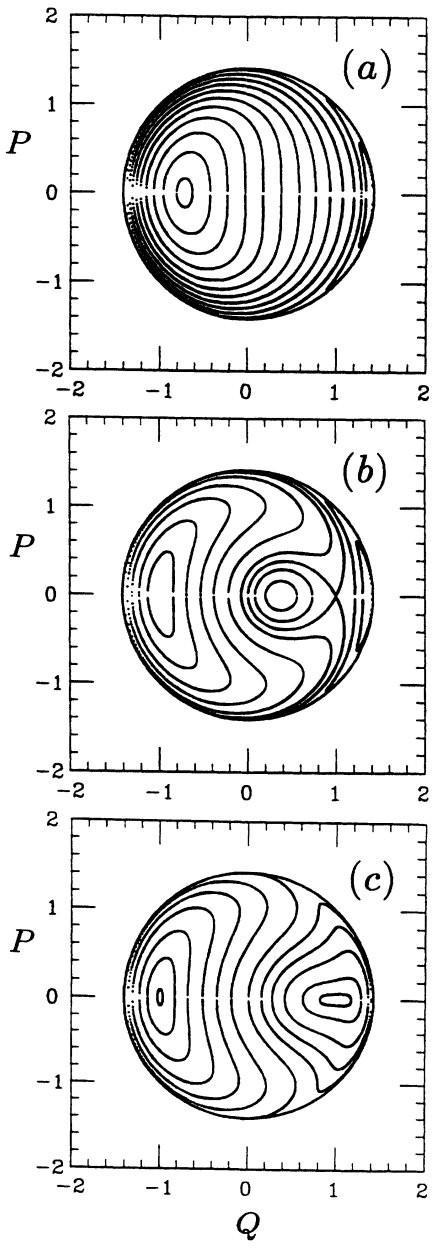

FIG. 1. The invariant tori of the 2D linearly coupled Hamiltonian with parameters (a) $b = 0$, $c = 0.25$; (b) $b = -0.5$, $c = 0.25$; and (c) $b = -0.5$, $c = 0.5$, respectively.

Solutions of Eq. (6) can be divided into two cases: (a) three stable fixed points (SFP's) and 1 unstable fixed point (UFP) [Fig. 1(b)] or (b) 2 SFP's [Figs. 1(a) and 1(c)]. Note particularly that $J_1 = J_2$ and $\phi_1 = \pm\frac{\pi}{2}$ are not the UFP of the Hamiltonian. The arc of $J_1 = J_2$ corresponds to $J_z = 0$ and vice versa, i.e., $J_1 = 0$ is equivalent to $J_z = J_2$.

The number of fixed points depends on the parameters b and c. The "square" symbol of Fig. 2 shows the critical coupling resonance strength c_b as a function of the parameter b. When the parameter b lies between $[-1, 0]$ and $|c| \leq c_b$, there are four fixed points. Figure 1(b) shows an example of having four fixed points and Fig. 1(c) shows an example that three fixed points have just merged together to form a single SFP at $x_{\rm SFP} = 0.5$ with $b = -0.5$ and $c = c_b = 0.5$. The corresponding coupling strength c_b is called the *bifurcation* coupling resonance strength. As $|c|$ approaches c_b from below, two fixed points (1 SFP and 1 UFP) on the $\phi_1 = 0$ axis are merging and vanishing. If the sign of c is reversed, all tori shown in Fig. 1 will be reflected with respect to the vertical axis. The bifurcation resonance strength exhibited a symmetry with respect to the value $b = -\frac{1}{2}$. This symmetry is equivalent to expanding the resonant rotating frame around the vertical action. The diamond symbols in Fig. 2 show the transition resonance strength, c_t, where the torus passing through $J_1 = J_2$ is also the separatrix. When $|c| > c_t$, the torus, which describes the particle motion for a beam kicked horizontally, will intercept the $\phi_1 = 0$ or π axis at a coordinate inside the UFP. This marks a possible sizable exchange of the horizontal and the vertical actions.

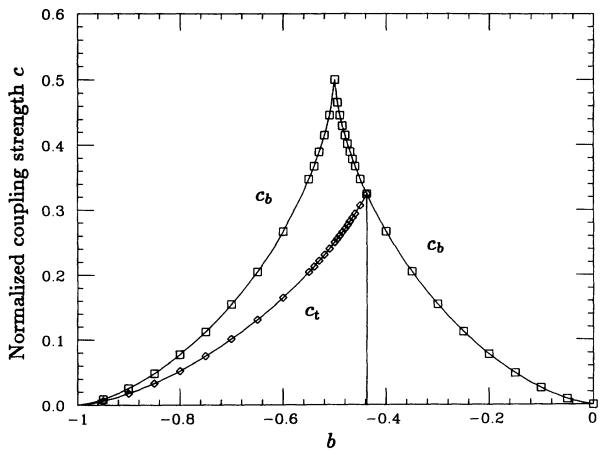

FIG. 2. The normalized bifurcation resonance strength c_b (squares) and the transition resonance strength c_t (diamonds) are plotted as a function of the normalized resonance proximity parameter b. Note here that c_b is symmetric with respect to $b = -\frac{1}{2}$. Similar symmetry can be obtained for c_t.

A. Small nonlinear detuning limit

In the limit that $\alpha_{11} = 0$, the SFP's of the Hamiltonian are

$$J^{\pm}_{1,\rm SFP} = \frac{\lambda \pm \delta_1}{2\lambda} J_2, \quad \lambda = \sqrt{\delta_1^2 + C^2}, \tag{7}$$

at $\phi_1 = 0$ and π respectively. Particles located initially at the SFP's of the Hamiltonian have the betatron oscillations which are correlated in phase without an exchange of betatron amplitudes. Particle motion is divided into two halves by the resonant curve $C\sqrt{J_1}\cos\phi_1 = \delta_1\sqrt{J_2 - J_1}$.

Using Hamilton's equations [Eqs. (4) and (5)], one obtains

$$\ddot{J}_1 + \lambda^2 J_1 = \lambda^2 \bar{J}, \tag{8}$$

where $\bar{J} = (2\delta_1 E + C^2 J_2)/2\lambda^2$ with the energy $E = \delta_1 J_1 + C\sqrt{J_1(J_2 - J_1)}\cos\phi_1$. Thus the evolution of the action at a linear coupling resonance is sinusoidal, given by

$$J_1 = \sqrt{\bar{J}^2 - E^2/\lambda^2}\cos[\lambda\theta + \varphi] + \bar{J}, \tag{9}$$

where $|E| \leq \lambda\bar{J}$, φ is an initial phase factor. Thus the "island" tune of the coupling oscillation for any torus is equal to λ, which is independent of the amplitude. Thus the orbiting periods are identical for all tori of the Hamiltonian. For a given bunch distribution with identical betatron tune, the bunch shape will return to its original bunch shape after $\frac{1}{\lambda}$ turns. Particles with different betatron tunes will be orbiting around different fixed points at different island tunes.

B. Evolution equation with nonzero detuning

In the case where $\alpha_{11} \neq 0$, the period of the linear coupling oscillation for a torus at constant J_2 and constant energy $H_1 = E$ is given by

$$\int d\theta = \frac{2}{\alpha_{11}J_2}\oint \frac{dx}{\sqrt{-\left[x^4 + 4bx^3 + 4\left(a^2 - \frac{E}{\alpha_{11}J^2}\right)x^2 - 8a^2\frac{\bar{J}}{J_2}x + 4\left(\frac{E}{\alpha_{11}J_2^2}\right)^2\right]}}. \tag{10}$$

There are possibly four or two roots for the denominator of Eq. (10) for a given energy E. The integral of Eq. (10) is independent of the specific pairs of turning points. This means that particle orbits with the same energy E have identical frequency orbiting about different SFP's. The minimum splitting between normal modes depends in general on both $\alpha_{11}J_2$ and C. Similarly, the equation of motion for J_1 is given by

$$\ddot{J}_1 + (\lambda^2 - \alpha_{11}E)J_1 + \frac{3}{2}\alpha_{11}\delta_1 J_1^2 + \frac{1}{2}\alpha_{11}^2 J_1^3 = \bar{J}. \quad (11)$$

In the limit $\alpha_{11}J_2\delta_1 \ll \lambda^2$, $(\alpha_{11}J_2)^2 \ll \lambda^2$, and $\alpha_{11}E \ll \lambda^2$, then the betatron tune separation of two normal modes becomes λ.

III. EXPERIMENTAL METHOD AND DATA ANALYSIS

The experiment started with a single bunch of about 5×10^8 protons with a kinetic energy of 45 MeV at the Indiana University Cyclotron Facility (IUCF) Cooler Ring. The cycle time was 10 s, and the injected beam was electron cooled for about 3 s before the measurement, producing a full-width at half-maximum bunch length of about 9 m (or 100 ns) depending on the rf voltage. The rf system used in the experiment was operating at the harmonic number $h = 1$ with frequency 1.0309 MHz.

To study the linear coupling, the horizontal and vertical betatron tunes are adjusted close to the resonance line, i.e., $\nu_x - \nu_z = -1$ with $\nu_x = 3.826, \nu_z = 4.817$. The coherent betatron oscillation of the beam is excited by a transverse dipole kick with a 600-ns flat top. The subsequent bunch transverse oscillations are detected and recorded. The experimental hardware has been reported earlier [4].

Figure 3 shows a typical example of the beating oscillations due to the linear betatron coupling following a horizontal kick. The beat periods were measured to be about 120 turns. We obtained $\lambda \approx 0.0083$ for this data set. The linear coupling in the IUCF Cooler Ring arose mainly from the solenoid at the electron cooling section, and possibly also from quadrupole roll and vertical closed-orbit deviations in sextupoles. The Lambertson septum magnet at the injection area also contributed a certain amount of skew quadrupole field, which was locally corrected.

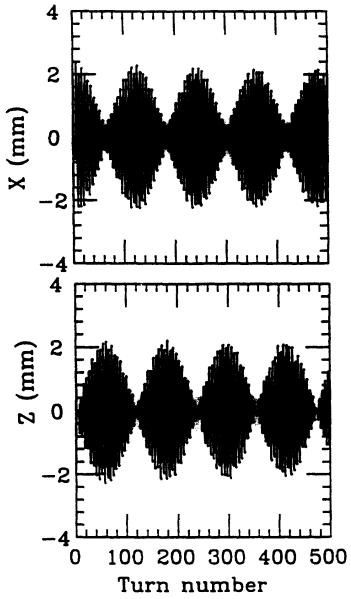

FIG. 3. The measured coherent betatron oscillations excited by a horizontal kicker. The linear coupling gives rise to the beating between the horizontal and vertical betatron oscillations.

The linear coupling resonance is usually corrected by maximizing the beat period of the transverse oscillations using a pair, or at least two families, of skew quadrupoles. Figure 4 shows the output from a spectrum analyzer using the difference (Δ) signal of a horizontal beam position monitor (BPM) as the input. The spectrum analyzer was tuned to a horizontal betatron sideband and was triggered 1.5 ms before the beam was coherently ex-

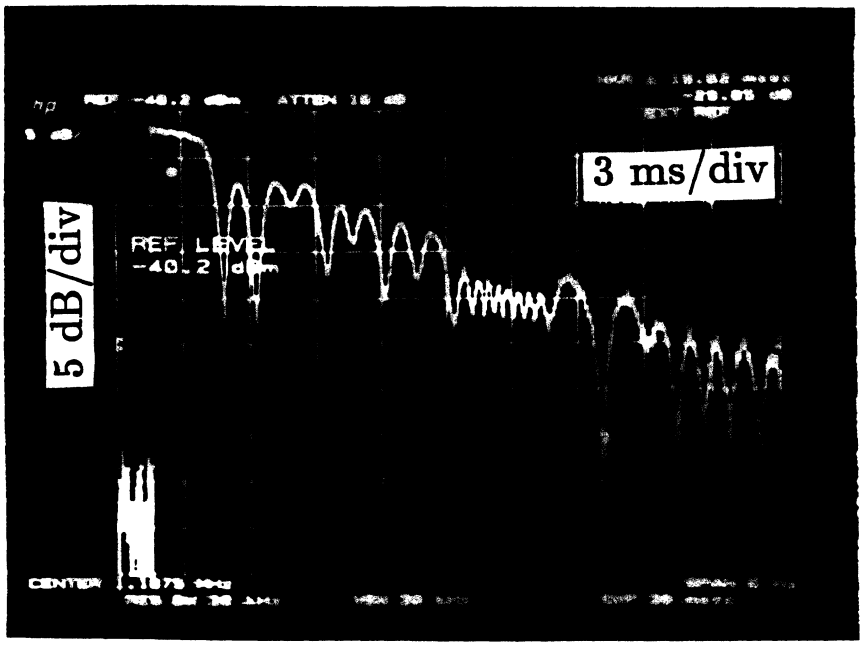

FIG. 4. The spectrum of the Δ signal from a horizontal BPM was shown from a spectrum analyzer tuned to a betatron sideband frequency with resolution bandwidth of 30 kHz triggered at 1.5 ms before a coherent horizontal kick. Note here that (1) the time interval between these dips corresponded to the beat period of Fig. 3, (2) the decay of the power spectrum corresponded to betatron decoherence, and (3) the characteristic change in feature at a 17-ms interval corresponded to a strong 60-Hz ripple, which altered betatron tunes.

cited by a horizontal kicker. The beat period shown in Fig. 3 corresponds to the time interval between the dips of Fig. 4.

The procedure for the linear coupling correction usually proceeds as follows: (1) maximize the peak to valley ratio in the spectrum by using quadrupole combinations and (2) maximize the time interval between dips (or peaks) of the spectrum by using families of skew quadrupoles. Repeated iteration of the above steps can efficiently correct the linear coupling, provided that these skew quadrupole families have proper phase relations. This procedure is however hindered by the betatron decoherence and by the 60-Hz power supply ripple, which is evident in Fig. 4. Other possible complications are closed-orbit changes due to off-center orbits in the quadrupoles and skew quadrupoles. However, the most important issue is that there is no guarantee *a priori* that the set of skew quadrupoles can correct the magnitude and the phase of the linear coupling. Thus measurement of the coupling phase is also important.

To measure the linear coupling phase χ, we can transform the horizontal and the vertical Poincaré maps into the resonant rotating frame discussed in Sec. II. Figure 5 shows the normalized phase space x, p_x and z, p_z of the data shown in Fig. 3. Because of the linear coupling between the horizontal and the vertical betatron oscillations, the horizontal and vertical phase spaces were completely smeared. Transforming the phase space into the resonant rotating frame, the torus of the 2D Hamiltonian is shown in Fig. 5(c), where the Courant-Snyder invariant circle and the resonant curve are clearly visible. The orientation of the resonant line was used to determine the coupling phase $\chi = 1.59$ rad, where the relative betatron phase advances at the locations of the horizontal and vertical BPM's were included. The action J_1 as a function of time and its time derivative, $\frac{dJ_1}{dN} = 2\pi \dot{J}_1$, were plotted in Fig. 6, where a five-point moving average of J_1 was used to obtain a better behaved time derivative of the action J_1. The time derivative, $\frac{dJ_1}{dN}$, was fitted with Eq. (4) to obtain $C = 0.0078 \pm 0.0006$, shown as a solid line in the lower graph of Fig. 6. Once C and χ were known, one used the torus of Fig. 5(c) to determine the parameters $\alpha_{11} = 0.001 \pm 0.0005$ $(\pi\text{-mm-mrad})^{-1}$ and $\delta_1 = -0.0016 \pm 0.0005$. The percentage errors for the determination of δ_1 and α_{11} were considerably larger. Nevertheless, the resulting $\lambda \approx 0.008 \pm 0.001$ agreed reasonably with the beat period observed in Fig. 3.

Figure 7 shows two invariant tori with an identical skew

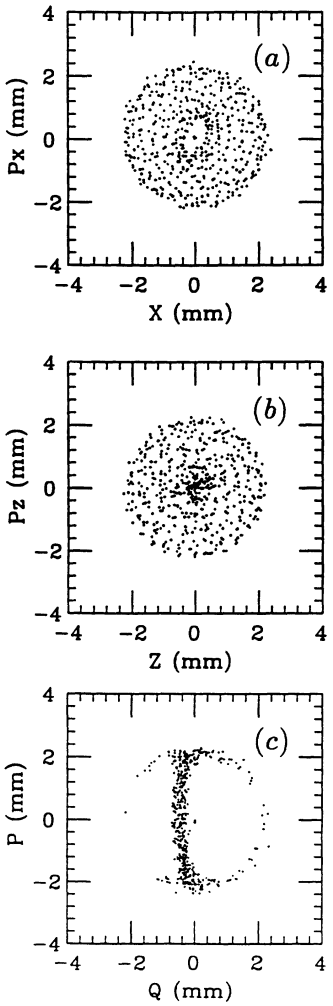

FIG. 5. The top two graphs show the observed Poincaré maps in (x, p_x), (z, p_z) of Fig. 1. The Poincaré map in the resonant precessing frame derived from top two graphs is shown at the bottom, where $Q = \sqrt{2J_1\beta_x}\cos\phi_1$ and $P = -\sqrt{2J_1\beta_x}\sin\phi_1$ with $\beta_x = 7.55$ m are used for this figure. The resonance phase was properly added to obtain the torus in the upright position.

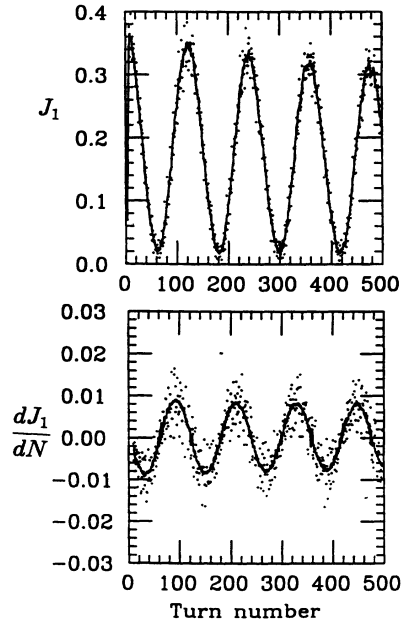

FIG. 6. The action J_1 (top) in (π-mm-mrad) and its time derivative, $\frac{dJ_1}{dN}$ (bottom) in (π-mm-mrad)/turn, were plotted as a function of time in orbital turns. The solid line in the top graph corresponded to a five-point running average of the action. The solid line in the bottom graph corresponded to a fit by using Eq. (4) to obtain the coupling strength $C = 0.0078$ and the coupling phase $\chi = 1.59$ rad.

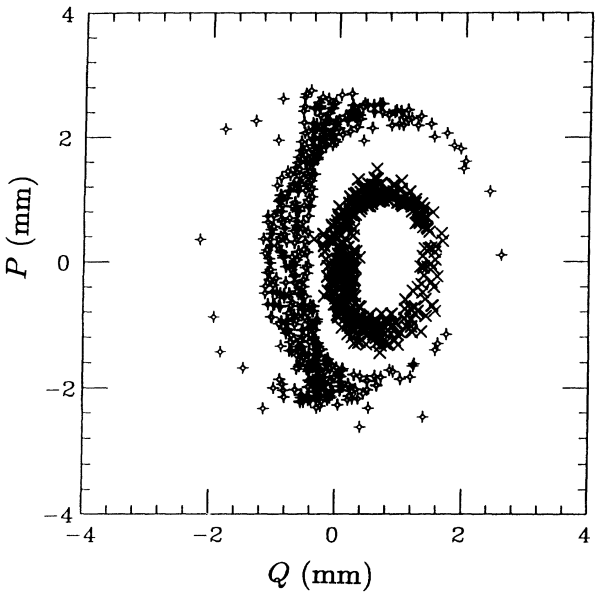

FIG. 7. Tori of the 2D Hamiltonian close to a linear coupling resonance condition were obtained from experimental measurements with identical skew quadrupole strengths. The outer torus corresponded to a purely horizontal kick and the inner torus corresponded to both horizontal and vertical kicks. Again, $Q = \sqrt{2J_1\beta_x}\cos\phi_1$ and $P = -\sqrt{2J_1\beta_x}\sin\phi_1$ with $\beta_x = 7.55$ m are used for this figure.

quadrupole strength at different initial betatron amplitudes similar to that of Fig. 1. The outer curve corresponded to a torus with horizontal kick only and the inner curve corresponds to a torus with both horizontal and vertical kicks. The beat periods were 333 and 384 revolutions, respectively. The fact that the beat periods of these two tori were close to each other was another indication that the nonlinear detuning parameter α_{11} was small. The measured Poincaré maps indeed exhibited Hamiltonian flow similar to that of Fig. 1.

IV. CONCLUSION

We found that the linear coupling in the presence of nonlinear detuning exhibited intricate stable and unstable fixed points of a Hamiltonian system. The Poincaré map derived from experimental data at a 2D linear coupling resonance showed invariant tori of the Hamiltonian flow. Using these invariant tori and Hamilton's equations of motion, the magnitude and the phase of the linear betatron coupling were determined. The magnitude of the linear coupling obtained from the invariant tori agreed well with that obtained from the traditional method of finding the minimum separation of the betatron tunes with combinations of quadrupole strengths. In a single digitized measurement, one could obtain the magnitude and the phase of the linear coupling. Such a correction method can be used for an on-line diagnosis system in order to choose more efficiently proper skew quadrupole correction families.

Knowing the dynamics of the linear coupling of a single-particle motion may also help to unravel questions concerning the dynamical evolution of the bunch distribution when the betatron tunes ramp through a coupling resonance. Such a problem is important for the polarized-proton acceleration in a low to medium energy synchrotron, where the vertical betatron tune jump method is necessary in order to overcome intrinsic depolarizing resonances. When the betatron tunes cross each other adiabatically after the tune jump, the increase in the vertical emittance due to linear coupling may cause difficulty in later stages of polarized proton acceleration [5].

ACKNOWLEDGMENTS

We thank Dr. Leo Michelotti for helpful discussions. Work supported in part by a grant from National Science Foundation NSF PHY-9221402 and from the U.S. DOE DE-FG02-93ER40801.

[1] E.D. Courant and H.S. Snyder, Ann. Phys. **3**, 1 (1958).
[2] G. Guignard, CERN Report No. 76-06, 1976 (unpublished); J.P. Gourber *et al.*, in *Proceedings of the Second European Particle Acceleration Conference*, Nice, 1990, edited by P. Marin and P. Mandrillon (Editions Frontières, France, 1990), p. 1429; G. Guignard *et al.*, *ibid.*, p. 1432.
[3] D.A. Edwards and L.C. Teng, IEEE Trans. Nucl. Sci. **20**, 855 (1973).
[4] S.Y. Lee *et al.*, Phys. Rev. Lett. **67**, 3768 (1991); D.D. Caussyn *et al.*, Phys. Rev. A **46**, 7942 (1992); M. Ellison *et al.*, Phys. Rev. Lett. **70**, 591 (1993).
[5] S.Y. Lee, Phys. Rev. E **47**, 3631 (1993).

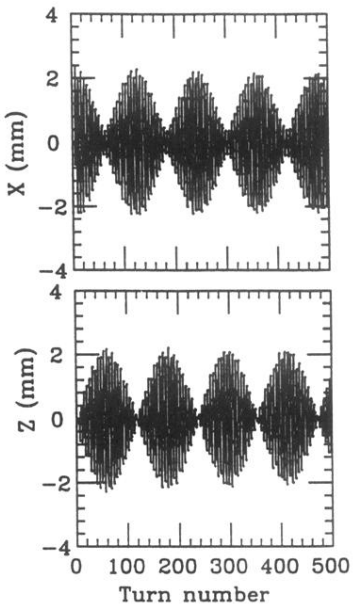

FIG. 3. The measured coherent betatron oscillations excited by a horizontal kicker. The linear coupling gives rise to the beating between the horizontal and vertical betatron oscillations.

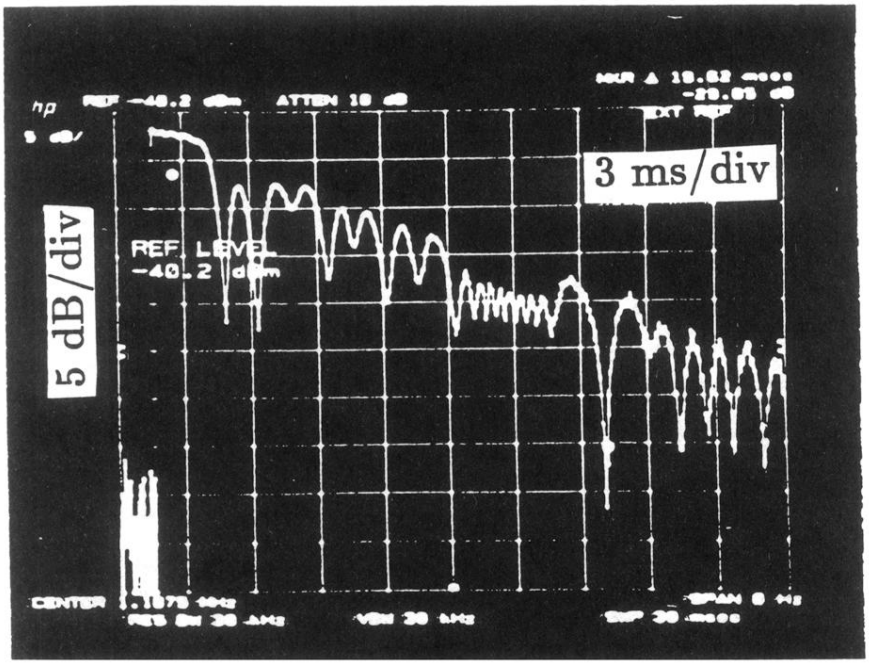

FIG. 4. The spectrum of the Δ signal from a horizontal BPM was shown from a spectrum analyzer tuned to a betatron sideband frequency with resolution bandwidth of 30 kHz triggered at 1.5 ms before a coherent horizontal kick. Note here that (1) the time interval between these dips corresponded to the beat period of Fig. 3, (2) the decay of the power spectrum corresponded to betatron decoherence, and (3) the characteristic change in feature at a 17-ms interval corresponded to a strong 60-Hz ripple, which altered betatron tunes.